Journal of the Franklin Institute 362 (2025) 108152

Contents lists available at ScienceDirect

Journal of the Franklin Institute

journal homepage: www.elsevier.com/locate/fi

Robust convergency indicator using MIMO-PI controller in the presence of disturbances ⋆

Zimao Sheng [a,b], Hong'an Yang [a,b,*], Jiakang Wang [a,b], Tong Zhang [a,b]

[a] School of Mechanical Engineering, Northwestern Polytechnical University 127 West Youyi Road, Beilin District, Xi'an, Shaanxi, 710072, PR China
[b] Key Laboratory of Industrial Engineering and Intelligent Manufacturing, 127 West Youyi Road, Beilin District, Xi'an, Shaanxi, 710072, PR China

ARTICLE INFO

Keywords:
Nonlinear disturbed system
MIMO proportional-integral control
Robust stability
Robust convergency indicator
Optimal parameter tuning

ABSTRACT

The PID controller remains the most widely adopted control architecture, with groundbreaking success across extensive implications. However, optimal parameter tuning for PID controller remains a critical challenge. Existing theories predominantly focus on linear time-invariant systems and Single-Input Single-Output (SISO) scenarios, leaving a research gap in addressing complex PID control problems for Multi-Input Multi-Output (MIMO) nonlinear systems with disturbances. This study enhances controller robustness by leveraging insights into the velocity form of nonlinear systems. It establishes a quantitative metric to evaluate the robustness of MIMO-PI controller, clarifies key theories on how robustness influences exponential error stabilization. Guided by these theories, an optimal robust MIMO-PI controller is developed without oversimplifying assumptions. Experimental results demonstrate that the controller achieves effective exponential stabilization and exhibits exceptional robustness under the guidance of the proposed robust indicator. Notably, the robust convergence indicator can also effectively assess comprehensive performance.

1. Introduction

1.1. Motivation

Classical proportional-integral-derivative (PID) control stands as the most fundamental and extensively utilized feedback - based control algorithm, being implemented in over 95% of control loops within engineering control systems [1]. Despite the advancements in advanced control techniques, PID control maintains its irreplaceable position [2]. This is attributed to its simple model-free structure and remarkable robustness in nullifying the impact of uncertainties. A plethora of enhanced PID controller versions [3] have notably improved their key performance indicators, particularly in terms of robustness, in the domains of industrial process control [4] and nonlinear optimization problems [5]. However, most of the current industrial systems exhibit characteristics such as Multi-Inputs and Multi-Outputs (MIMO), strong coupling of state variables, strong external disturbances, undesired sensor faults and actuator

⋆ This document is the results of the National Natural Science Foundation of China (Grant No.51775435), the pertinent preprint can be accessed via the following link https://arxiv.org/abs/2411.13140. Our experimental code is available at: https://github.com/Dr-A-Mao/Robust-convergency-indicator-using-MIMO-PI-controller-in-the-presence-of-disturbances.git.

* Corresponding author.
E-mail addresses: hpShengZimao@163.com (Z. Sheng), yhongan@nwpu.edu.cn (H. Yang), wangjk@mail.nwpu.edu.cn (J. Wang), zhangt_@mail.nwpu.edu.cn (T. Zhang).

https://doi.org/10.1016/j.jfranklin.2025.108152
Received 10 February 2025; Received in revised form 17 July 2025; Accepted 11 October 2025
Available online 15 October 2025

faults. These features pose higher requirements for the design of a high-robustness PID controller with MIMO, nonlinearity, and anti-disturbance capabilities.

Consequently, a pertinent question emerges: How to gauge the robustness of PID controller parameters for general perturbed MIMO nonlinear systems to enable more effective and optimal parameter regulation for exponential stabilization? Classical approaches to regulating PID controller parameters have predominantly relied on practical experiments [6] and experiences like the Ziegler–Nichols rules [7]. For systems with specific structures, such as linear [8] or affine nonlinear [9] systems, the gain regulation process for the PID controller is often manageable. Nevertheless, exploring suitable parameters for general nonlinear systems is usually complex as the corresponding search space is typically vast.

Although there have been studies exploring methods to ensure the exponential stabilization of uncertain systems through appropriate PID parameter regulation [10–12], the current research emphasis still primarily lies in maintaining the asymptotic regulation of systems rather than enhancing the robustness capacity. Besides, the control mechanism by which a PID controller can control MIMO nonlinear systems with disturbances remains unclear, impeding the implementation of a regulation method that can effectively guarantee robust stability. Moreover, the application of the theoretical results [10] to practical parameter adjustment, and designing controllers applicable to MIMO nonlinear systems in a general form and with more general disturbances remains a formidable challenge. These circumstances have motivated us to consider the optimal parameter regulation of general perturbed MIMO systems to fortify the controller's robustness in the presence of disturbances.

1.2. Related work

The concept of addressing uncertainty using the infinity norm, known as H_∞ control [13], has ultimately been specialized to the case of robust PID control. In traditional robust PID control parameter tuning, frequency-domain internal model control (IMC) [14,15] is most commonly employed in linear Single-input and Single-output (SISO) systems. This is based on numerous variants of setting the gain and phase margin [16], as well as other flexible extensions that directly parameterize the maximum of the sensitivity function [17]. For nonlinear SISO systems, criteria such as the Popov criterion need to be considered when designing an appropriately robust stabilization utility [18]. However, for a long time, a MIMO PID controller capable of stabilizing general nonlinear perturbed state-space-based systems has been absent. Additionally, manual PID parameter regulation undermines the controller's robustness, causing it to deviate from its optimal state and offering no guarantee of process stability [19]. Meanwhile, the explicit design formulas for PID parameters in the context of MIMO systems to globally stabilize the regulation error, along with theoretical insights relevant to a class of nonlinear, uncertain stochastic systems, are presented in [20–22].

We analyze and discuss representative studies on PID controller design for MIMO systems over the past five years, as summarized in Table 1. Current mainstream MIMO-PID controllers are predominantly developed for linear systems [23,25–28], and most of these controllers lack investigations into the influence mechanism of disturbance factors and considerations of post-disturbance robustness [25,26]. For the majority of existing MIMO-PID controllers tailored to nonlinear systems, overly complex theoretical frameworks restrict their applicability to specific forms of affine nonlinear systems [29–31]. Moreover, the design of MIMO-PID controllers for most disturbed nonlinear systems lacks theoretical guarantees of robust stability [24,29]. Furthermore, all the aforementioned studies have not thoroughly explored critical questions: What factors in MIMO-PID controllers affect the system's robust stability? How can the robust stability margin in this process be precisely and meticulously quantified via controller coefficients? These key issues necessitate in-depth research within a complex theoretical framework.

Theoretically, Cheng [20] and Guo [10] both derived sufficient conditions for ensuring effective error stabilization in PID controller. Specifically, controller parameters are constrained within a range linked to the Lipschitz constant of the nonlinear system's mapping. However, obtaining such a Lipschitz constant is typically challenging, which impedes practical implementation. Cheng [11] developed a PID controller by integrating high-order differential terms of the error. However, this focus often results in limited adaptability for stochastic systems affected by bounded perturbations. The underlying reason is the absence of customized robust indicators. Therefore, in this paper, a novel robustness criterion and an optimal fine-tuning for adaptive MIMO Proportional-Integral (MIMO-PI) controller parameter regulation methods are proposed, which ensures robust stability.

1.3. Contributions

The main contributions are as follows

- First, we innovatively established sufficient conditions for the robust stabilization of general disturbed autonomous nonlinear systems, alongside determining the specific exponential convergence rate and the range of the global random attractor. This forms a theoretical framework for subsequent quantification of key indicators of MIMO-PI controllers, as detailed in Theorem 1;
- Next, from the perspective of the velocity form, we analyzed the sufficient conditions for exponential convergence in disturbed nonlinear systems driven by MIMO-PI controllers (see Theorem 2). Using the controller coefficients, we quantified both the exponential convergence rate and the scope of the global random attractor, yielding the critical robust convergence indicators R_K and I_K. These indicators were modeled as an eigenvalue problem (EVP), with specific calculation methods provided in Eqs. (51) and (52);
- Finally, building upon the aforementioned theory, we proposed a controller parameter optimization model that satisfies input constraints, as presented in Eq. (53). Experimental results validate the rationality of the indicators and the optimality of the optimization model.

Table 1
A comparative analysis is conducted on some representative MIMO-PID controllers in the recent 5 years.

Refs	Systems	Disturbances	Methods	Limitations
Yu [23]	MIMO Linear Time-Invariant (LTI) systems with multiple time delays	Multiple time delays	Calculation of stabilizing regions for low-order controllers, decomposition of MIMO systems using Equivalent Transfer Function (ETF)	Limited to LTI systems, don't not discusse the robust stabilization strategies under uncertain time-delay parameters
Wang [24]	MIMO Nonlinear systems with time-varying uncertainty	Time-varying uncertainty	Formulates a deep Reinforcement Learning (RL), IDDPG, based adaptive PID tuning strategy to track setpoints	A significant consumption of training time and a lack of theoretical robust stability guarantees
Pandey [25]	MIMO LTI systems, square, time-delayed, and non-square non-minimum phase configurations	None	Uses enhanced PID method utilizing the Kharitonov theorem, the linear matrix inequality (LMI) approach is commonly utilized to successfully mitigate the coupling effects between input and output of systems	Limited to LTI systems, a lack of consideration for robust stability against disturbances
Ben [26]	MIMO LTI systems	None	Examines the potential of various artificial bee colony (ABC) algorithm variants for optimizing the design of fractional-order Proportional Integral and Derivative controllers	A significant consumption of optimization time and a lack of theoretical robust stability guarantees
Cavanini [27]	MIMO discrete LTI plant	Actuator fault with input saturation constraints	Uses Adaptive Kalman Filter (AKF) for optimal fault estimation, replace conventional Anti-Windup (AW) schemes for PIDs, and LMI conditions for the local stability	Limited to LTI systems, a lack of consideration for robust stability against disturbances
Gopmandal [28]	MIMO Linear System Time-Variant (LTV) systems	Norm-bounded time-varying parametric uncertainties within norm-bounded, time-varying, uncertain matrices	A hybrid search based method for H_∞ synthesis of LTI static output feedback (SOF) controllers, using a new sufficient condition in terms of LMIs for existence of SOF to improve robust stability	Limited to linear system, constrained by specific bounded disturbances and the form of state matrices
Zhong [29]	MIMO non-affine uncertain systems	Model uncertainy with an upper bound on the Jacobians	Active disturbance rejection control (ADRC) based tuning rule to disturbance-free PID, derive large-scale robustness conditions with respect to uncertainties and enable decoupling control	A lack of consideration for robust stability against bounded stochastic disturbances on the differential of the states
Xiang [30]	Non-square MIMO nonlinear affine feedforward-like systems	Time-varying yet uncertain control gain matrix, unknown and possibly time-varying parameter	Incorporates three nonlinear modulating functions to recalibrate generalized tracking error, integrates adaptive single-parameter tuning to avoid manual trial-and-error while ensuring bounded comprehensive performance under nonlinearities and uncertainties	Limited to a specific class of high-order MIMO nonlinear systems with normal form-like structures, limiting its direct applicability to more general nonlinear system types (e.g., non-normal form systems); excessively rely on user-adjustable parameters, potentially complicating practical implementation
Zhu [31]	A class of MIMO affine nonlinear system	Model uncertainties encompassing unmodeled dynamics and perturbations	For a class of MIMO strongly coupled nonlinear uncertain systems with mixed relative degrees	Restricted to MIMO systems with mixed relative degrees one and two, a lack of explicit external disturbances (e.g., bounded stochastic or time-varying disturbances)

This paper is organized as follows. After an overview in Section 1, the numerous theoretical results regarding the robustness of nonlinear perturbed systems intended for subsequent optimal MIMO-PI controller is given in Section 2, and the perturbed model and constrained input commands, along with the problem formulation, is presented in Section 3. The proposed robust convergency indicator and optimal MIMO-PI controller are designed in Section 4, and simulation verification experiments in Section 5. Finally, we present concluding remarks and directions for future investigation in Conclusions and future work.

2. Preliminaries

In this section, we present several key definitions, lemmas, and theorem as essential tools for subsequent analyses.

2.1. Notations and definitions

Denote $\mathbb{R}^n$ as the n-dimensional Euclidean space, $\mathbb{R}^{m\times n}$ as the space of $m\times n$ real matrices, $||x||_2 = x^T x$ as the Euclidean 2-norm of a vector x. The norm of a matrix $P \in \mathbb{R}^{m\times n}$ is defined by $||P||_2 = \sup_{x\in R^n, ||x||_2=1} ||Px||_2 = \sqrt{\lambda_{\max}(P^T P)}$, for given matrix set $\mathbb{P}$, its 2-norm is defined as $||\mathbb{P}||_2 = \arg\sup_{P\in\mathbb{P}} ||P||_2$, $\sigma_{\min}(P) = \sqrt{\lambda_{\min}(P^T P)}$. We denote $Res(J)$ as the real part of the eigenvalues associated with matrix J, besides $\lambda_{\min}(S)$ and $\lambda_{\max}(S)$ as the smallest and the largest eigenvalues of S,respectively. For a function $\Phi = (\Phi_1, \Phi_2, \dots \Phi_n)^T \in \mathbb{R}^n$,$x = (x_1, x_2, \dots x_m)^T \in \mathbb{R}^m$, let $\frac{\partial \Phi}{\partial x^T} = (\frac{\partial \Phi_i(x)}{\partial x_j})_{ij}$. Matrix $A < B$ means $A - B$ is negative define matrix.

Definition 1 (Robust stability). For perturbed nonlinear system $\dot{y} = f(t,y) + g(t,y),\ y \in \mathbb{R}^n, f(t,0) = 0,\ f, g \in C[I \times S_H, \mathbb{R}^n], S_H = \{x | ||x||_2 \le H\}$, if $\forall \varepsilon > 0$, there exists $\delta_1(\varepsilon) > 0$ and $\delta_2(\varepsilon) > 0$ to make $||g(t,y)||_2 \le \delta_1(\varepsilon)$, $||y(0)||_2 \le \delta_2(\varepsilon)$, and $||y||_2 \le \varepsilon$, then the trivial solution of $\dot{y} = f(t,y) + g(t,y), f(t,0) = 0$ exhibits robust stability.

Definition 2 (Global attractor). For a dynamical system: $\dot{x}(t) = f(x(t))$, $x(t) \in \mathbb{R}^n$, where $f : \mathbb{R}^n \to \mathbb{R}^n$ is a deterministic vector field (typically Lipschitz continuous). The set A for this state $x(t)$ is defined as the global attractor if $x(t) \notin A$, then the distance between $x(t)$ and A: $dist(x(t), A) \to 0$ as $t \to \infty$; if $x(t) \in A$, then $x(t + \Delta t) \in A$ for any $\Delta t \ge 0$.

Definition 3 (Global random attractor). For a dynamical system governed by a stochastic differential equation (SDE): $\dot{x} = f(x) + d$, $x \in \mathbb{R}^n$ and d is a stochastic perturbation. Its global attractor can be regarded as the global random attractor of the SDE.

Definition 4 (The exponential convergence rate of global random attractor). If there exists a constant $\lambda > 0$, and for non-empty bounded set $\mathcal{A}$ in X and all $t \ge 0$, for the trajectory $\varphi(t), \varphi(t_0) = \varphi_0$ of the disturbed dynamical system, the following holds:

$$dist_X(\varphi(t), \mathcal{A}) \le dist_X(\varphi_0, \mathcal{A}) e^{-\frac{\lambda}{2}t}$$

where $dist_X(\varphi(t), \mathcal{A})$ denotes the distance between the trajectory $\varphi(t)$ and the global random attractor $\mathcal{A}$, then the global random attractor $\mathcal{A}$ is said to have an exponential convergence rate of λ. A larger λ indicates a faster convergence speed of the system trajectory to the global random attractor $\mathcal{A}$.

2.2. Key lemmas and theorem

Lemma 1 (Stability of matrix [32]). *If A is stable, which means $Res(A) < 0$ or eigenvalue 0 corresponds to the single characteristic factor, there exists only one positive define $P = P^T = P(A,\delta) > 0$ for any $\delta > 0$ to make:*

$$P(A,\delta)A + A^T P(A,\delta) + \delta I = O \tag{1}$$

Lemma 2 (Weyl's inequality [33]). *In the context of matrix perturbation analysis, consider a symmetric matrix $A = A^T \in \mathbb{R}^{n\times n}$ and its perturbation $\Delta A = \Delta A^T \in \mathbb{R}^{n\times n}$. A fundamental result states that$\|\lambda_{\max}(A + \Delta A) - \lambda_{\max}(A)\|_2 \le \|\Delta A\|_2$,where $\lambda_{\max}(\cdot)$ denotes the maximum eigenvalue.*

Lemma 3. *For $f(x) \in \mathbb{R}^n$, if $f(x)$ is differentiable and β_f-Smoothness over the region $x \in \Omega \subset \mathbb{R}^n$ near $x = 0$, then there exists*

$$\left|\lambda_{\max}\left[\frac{\partial(f(x) + f(x)^T)}{\partial x}\right] - \lambda_{\max}\left[\frac{\partial(f(0) + f(0)^T)}{\partial x}\right]\right| \tag{2}$$
$$\le 2\beta_f ||x||_2$$

Proof. There exists

$$\left|\lambda_{\max}\left[\frac{\partial(f(x) + f(x)^T)}{\partial x}\right] - \lambda_{\max}\left[\frac{\partial(f(0) + f(0)^T)}{\partial x}\right]\right| \tag{3}$$
$$\le ||\frac{\partial(f(x) + f(x)^T)}{\partial x} - \frac{\partial(f(0) + f(0)^T)}{\partial x}||_2, (\textbf{Lemma 2}) \tag{4}$$
$$\le 2||\frac{\partial f(x)}{\partial x} - \frac{\partial f(0)}{\partial x}||_2, (\beta_f - Smoothness\ of\ f(x)) \tag{5}$$
$$\le 2\beta_f ||x||_2 \tag{6}$$

The proof is completed. □

Lemma 4. *Consider the function $f(x) = A(x)x$, where $x \in \mathbb{R}^n$, $f(x) \in \mathbb{R}^n$, and $A(x) \in \mathbb{R}^{n\times n}$. If $f(x)$ is differentiable at $x = 0$, the Jacobian at this point $\partial f(0)/\partial x = A(0)$.*

Proof. Let the ith component of the function $f(x) = (f_1(x), f_2(x) \dots f_n(x))^T$ is denoted as $f_i(x)$, $A(x) = [a_{ij}(x)]_{n\times n}$, the partial derivative of $f_i(x)$ with respect to x_k is:

$$\frac{\partial f_i(x)}{\partial x_k} = \sum_{j=1}^{n}\left[\frac{\partial a_{ij}(x)}{\partial x_k}x_j + a_{ij}(x)\frac{\partial x_j}{\partial x_k}\right] \tag{7}$$
$$= \sum_{j=1}^{n}\frac{\partial a_{ij}(x)}{\partial x_k}x_j + a_{ik}(x) \tag{8}$$

Thus, for any i, k there exists $\partial f_i(0)/\partial x_k = a_{ik}(0)$, the proof is completed. □

Lemma 5. *For a nonlinear system $\dot{x}(t) = f(x(t))$ with initial state $x(0) = x_0$, $f(0) = 0$, $x \in \mathbb{R}^n$, suppose there exists a positive definite function $V(x)$ for any nonzero x satisfying*

$$\dot{V}(x) + \alpha V(x) - \beta V^{\frac{1}{2}}(x) \leq 0 \tag{9}$$

where $\alpha > 0$, $\beta > 0$. Then for any state $x(t)$ there exists

$$V^{\frac{1}{2}}(x(t)) \leq \frac{\beta}{\alpha} + (V^{\frac{1}{2}}(x_0) - \frac{\beta}{\alpha})e^{-\frac{\alpha}{2}t} \tag{10}$$

Proof. We define $s(t) = V^{\frac{1}{2}}(x)$, and then Eq. (9) can be transformed into

$$\dot{s}(t) + \frac{\alpha}{2}s(t) \leq \frac{\beta}{2} \tag{11}$$

The above equation can be further transformed into

$$e^{\frac{\alpha}{2}t}\dot{s}(t) + \frac{\alpha}{2}e^{\frac{\alpha}{2}t}s(t) \leq \frac{\beta}{2}e^{\frac{\alpha}{2}t} \tag{12}$$

which means

$$\frac{d}{dt}(e^{\frac{\alpha}{2}t}s(t)) \leq \frac{\beta}{2}e^{\frac{\alpha}{2}t} \tag{13}$$

Integrating both sides of the inequality in the above equation from 0 to t simultaneously, we can obtain

$$e^{\frac{\alpha}{2}t}s(t) - s(0) \leq \frac{\beta}{\alpha}(e^{\frac{\alpha}{2}t} - 1) \tag{14}$$

Therefore, the above equation can be further derived to obtain Eq. (10). Thus, the proof is completed. □

Remark 1. Eq. (10) reveals a fact that, when the initial value x_0 satisfies $V^{\frac{1}{2}}(x_0) \leq \frac{\beta}{\alpha}$, $V^{\frac{1}{2}}(x(t)) \leq \frac{\beta}{\alpha}$ holds for all $t \geq t_0$. Conversely, if $V^{\frac{1}{2}}(x_0) \geq \frac{\beta}{\alpha}$, $V^{\frac{1}{2}}(x(t))$ is upper - bounded by a function that converges exponentially to $\frac{\beta}{\alpha}$ with a rate of α. As t approaches infinity, once $V^{\frac{1}{2}}(t_r) \leq \frac{\beta}{\alpha}$ is satisfied at a certain time t_r, the trajectory of $x(t)$ will remain within this region indefinitely. Consequently, it can be deduced that for any initial value $x(t_0) = x_0$, $x(t)$ will ultimately converge to the region of attraction described as:

$$x(t) \in \{x | V^{\frac{1}{2}}(x) \leq \frac{\beta}{\alpha}\}, t \to \infty \tag{15}$$

It is worth noting that we generally aspire for the convergence rate α to be as large as possible. Meanwhile, a larger α also enables the scope of the final global random attractor, $\frac{\beta}{\alpha}$, to be minimized.

Theorem 1. *For the perturbed autonomous system $\dot{x} = f(x) + d$, where $x \in \mathbb{R}^n$, $x(t_0) = x_0$, $f(0) = 0$, and $d \in \mathbb{R}^n$ is the perturbation term satisfying $\|d\|_2 \leq L_d$. If there exists a Ω such that when $x \in \Omega$, the following conditions hold:*

1) There exists $L_f(\Omega) \geq 0$ such that $\left\| \frac{\partial f(x)}{\partial x} \right\|_2 \leq L_f(\Omega)$;

2) There exist a positive-definite matrix $P = P^T > 0$ and $\varepsilon(\Omega) > 0$ such that $\left[\frac{\partial f(x)}{\partial x} \right]^T P + P \frac{\partial f(x)}{\partial x} + \varepsilon(\Omega) I \leq O$.

Then the ultimate trajectory of the state $x(t)$, for any initial value x_0, $x(t)$ will exponentially converge to the following global random attractor $S(\Omega)$ at least the rate of $\varepsilon(\Omega)/\lambda_{\max}(P)$:

$$x(t) \to S(\Omega) = \{x : ||f(x)||_2 \leq \frac{2L_d L_f(\Omega)\lambda_{\max}^2(P)}{\varepsilon(\Omega)\lambda_{\min}(P)}\}, t \to \infty \tag{16}$$

Simultaneously, for any $x_0 \notin S(\Omega)$, $x(t)$ will converge exponentially to $S(\Omega)$ at a rate of $\varepsilon(\Omega)/\lambda_{\max}(P)$.

Proof. We construct the Lyapunov function

$$V(x) = f(x)^T P f(x) \tag{17}$$

such that

$$\begin{aligned}
\dot{V}(x) =& \dot{f}(x)^T P f(x) + f(x)^T P \dot{f}(x) \\
=& \dot{x}^T [\frac{\partial f(x)}{\partial x}]^T P f(x) + f(x)^T P [\frac{\partial f(x)}{\partial x}]\dot{x} \\
=& f(x)^T ([\frac{\partial f(x)}{\partial x}]^T P + P \frac{\partial f(x)}{\partial x}) f(x) \\
&+ d^T [\frac{\partial f(x)}{\partial x}]^T P f(x) + f(x)^T P \frac{\partial f(x)}{\partial x} d \\
\leq& -\frac{\varepsilon(\Omega)}{\lambda_{\max}(P)} V(x) + 2d^T [\frac{\partial f(x)}{\partial x}]^T P f(x) \\
\leq& -\frac{\varepsilon(\Omega)}{\lambda_{\max}(P)} V(x) + 2L_d ||\frac{\partial f(x)}{\partial x}||_2 ||Pf(x)||_2 \\
\leq& -\frac{\varepsilon(\Omega)}{\lambda_{\max}(P)} V(x) + \frac{2L_d L_f(\Omega)\lambda_{\max}(P)}{\sqrt{\lambda_{\min}(P)}} V(x)^{\frac{1}{2}}
\end{aligned} \tag{18}$$

According to the Lemma 5 and Remark 1, as $t \to \infty$,

$$V^{\frac{1}{2}}(x) \leq \frac{2L_d L_f(\Omega)\lambda_{\max}^2(P)}{\varepsilon(\Omega)\sqrt{\lambda_{\min}(P)}} \tag{19}$$

Consequently, as $t \to \infty$,

$$||f(x)||_2 \leq \frac{V^{\frac{1}{2}}(x)}{\sqrt{\lambda_{\min}(P)}} \leq \frac{2L_d L_f(\Omega)\lambda_{\max}^2(P)}{\varepsilon(\Omega)\lambda_{\min}(P)} \tag{20}$$

The proof is completed. □

Theorem 1 elucidates a pivotal theoretical framework. Let Ω be a non-empty subset of the state space $\mathbb{R}^n$ that encompasses the origin. When the Jacobian of the function $f(x)$, denoted as $J_f(x) = \partial f(x)/\partial x$, is uniformly bounded for all x within the domain Ω, and $J_f(x)$ exhibits negative definiteness throughout this region, the following property emerges for the associated dynamical system. For an autonomous dynamical system governed by the differential equation $\dot{x}(t) = f(x(t)) + d$, regardless of the chosen initial condition $x_0 \in \mathbb{R}^n$, in the absence of external perturbations, the time-derivative of the state trajectory $f(x(t))$ converges exponentially to the region of attraction as delineated in Eq. (16). The spatial extent of this region of attraction is intricately linked to two critical parameters: the supremum $L_f(\Omega)$ of the norm of the Jacobian matrix $J_f(x)$ over the domain Ω, and the upper bound $-\varepsilon(\Omega)$ of the maximum eigenvalue of $J_f(x)$ within Ω. Specifically, a smaller upper bound for the ultimate global random attractor $\|f(x)\|_2$ can be achieved through a smaller $L_f(\Omega)$ and a larger $\varepsilon(\Omega)$.

Remark 2. According to Lemma 1, there exists a sufficient condition for the validity of condition 2) in Theorem 1, specifically: when $x \in \Omega$, the Jacobian $\partial f/\partial x$ is stable. Furthermore, a special case arises when $\Omega = \{0\}$. In this scenario, determining whether $\partial f(0)/\partial x$ satisfies conditions 1) and 2) suffices to characterize the global random attractor $S(0)$ of the perturbed system's trajectory.

Remark 2 establishes the following theoretical principle: if the Jacobian matrix $\partial f/\partial x$ of $f(x)$ is continuously bounded and stable over a region $x \in \Omega$, then the trajectory $x(t)$ of the perturbed system will exponentially converge to a global random attractor in which the fluctuation amplitude of $f(x)$ remains bounded. Notably, the extent of this global random attractor is governed by the eigenvalues of $\partial f/\partial x$-larger eigenvalue magnitudes generally correspond to a smaller constrained domain, thereby enabling the system to attain a higher level of robust stability.

3. Problem formulation

In this section, based on Section 2, we analyze a general perturbed nonlinear system and propose a optimal MIMO-PI controller for optimizing its robustness near the origin. This method transforms the robustness optimization problem on a global scale into a special type of eigenvalue optimization problem at the origin, which can then be efficiently solved using classical methods.

Consider the following perturbed autonomous MIMO non-affine nonlinear system within continuous and first-order differentiable $f \in \mathbb{R}^n$ and first-order differentiable disturbance $d \in \mathbb{R}^n$

$$\begin{cases} \dot{x}(t) = f(x(t), u(t)) + d \\ y(t) = h(x(t)) \\ x(0) = x_0, f(0) = 0 \end{cases} \tag{21}$$

where state $x(t) \in \mathbb{R}^n$, control input $u(t) \in \mathbb{R}^m$, observable $y(t) \in \mathbb{R}^L$. The disturbance $d \in \mathbb{R}^n$ is a perturbation term independent of the state $x(t)$, it is only related to time t and can be either random noise or a time-dependent function, which has an upper bound on its amplitude as follows

$$||\dot{d}||_2 \leq L_d \tag{22}$$

It is recognized that, when random disturbances are present, errors in the vicinity of the origin are ultimately inescapable.

Nevertheless, our objective is to devise a suitable controller that, upon its application for any initial state x_0 and region Ω, minimizes the terminal-state error in the neighborhood of the origin, which aims to make the controlled variable $x(t)$ converge to the vicinity of desired reference value $x_r \in \mathbb{R}^n$ exponentially to the nearest extent possible. Specifically:

$$\min_u ||x(t)||_2, \ x(t) \in \Omega, \quad t \to \infty \tag{23}$$

In this context, we assume the existence of a state observer $h^{-1} : \mathbb{R}^L \to \mathbb{R}^n$, which is capable of delivering an exact state estimate $x(t) = h^{-1}(y(t))$ based on the current observable $y(t)$. This observer ensures that for every value of the observable quantity $y(t)$, the estimated state $x(t)$ precisely reflects the actual state of the system, thereby bridging the gap between the measured output and the internal states.

Further, we assume the adoption of a MIMO-PI controller that takes into account the coupling of multiple input channels. Explicitly,

$$u(t) = K_P x(t) + K_I \int_0^t x(t)dt \tag{24}$$

where $K_P \in \mathbb{R}^{m\times n}, K_I \in \mathbb{R}^{m\times n}$ and $x(t) = h^{-1}(y(t))$. Concurrently, the robustness optimization objective of Eq. (23), can be recast as an optimization task focused on determining the optimal values of the weights K_P, K_I. In what follows, we will elucidate the approach of leveraging the solution of a specific class of EVP to accomplish this goal. Here, the control commands and its first-order derivative quantity are constrained as

$$u_{\min} \le u(t) \le u_{\max}, \dot{u}_{\min} \le \dot{u}(t) \le \dot{u}_{\max} \tag{25}$$

where $u_{\min}, u_{\max}, \dot{u}_{\min}, \dot{u}_{\max}, \in \mathbb{R}^{m\times 1}$. We expect to exponentially stablize the Eq. (21) within maximum robust indicator to resist the emergency situation.

4. Controller for optimizing robust stability

Our objective is to minimize the ultimate value of the norm $\|x(t)\|_2$ for the controller designed based on Eq. (24). This goal corresponds to confining the state trajectory $x(t)$ to fluctuate within a narrow neighborhood around the origin. Leveraging the insights from Theorem 1, we are able to derive the sufficient conditions to meet our objective and solve it via classical optimization algorithms.

4.1. Theoretical foundation

The core theorems of this paper are presented below, which serve to characterize the relationship between the robust stability of the MIMO-PI controller and its coefficients.

Theorem 2. *For the perturbed autonomous system $\dot{x}(t) = f(x(t), u(t)) + d$, where $x(t) \in \mathbb{R}^n, x(t_0) = x_0$, $f(0) = 0$, and $d \in \mathbb{R}^n$ is the perturbation term satisfying $\|\dot{d}\|_2 \le L_d$, the MIMO-PI controller $u(x(t)) = K_P x(t) + K_I \int_0^t x(t)dt$, $K_P \in \mathbb{R}^{m\times n}, K_I \in \mathbb{R}^{m\times n}$ is adopted as the input. If the following conditions are satisfied:*

1) Here $f(x) = f(x, u(x))$ is differentiable at $x = 0$, there exists $L_f > 0$ such that

$$\left\| \frac{\partial f(0)}{\partial x} \right\|_2 \le L_f \tag{26}$$

and $f(x)$ is β_f-Smoothness near the origin;

2) Let

$$A_K(0) = \begin{pmatrix} \frac{\partial f(0)}{\partial x} + \frac{\partial f(0)}{\partial u} K_P & \frac{\partial f(0)}{\partial u} K_I \\ I_n & O \end{pmatrix} \tag{27}$$

Suppose appropriate values of K_P, K_I are chosen such that

$$Re\left[A_K(0)\right] < 0 \tag{28}$$

Then, the ultimate trajectory of the state $x(t)$, as $t \to \infty$, must converge exponentially to

$$s(t) = (x(t)^T, \dot{x}(t)^T)^T \to B(0, 2L_d L_f I_K) \tag{29}$$

with at least the rate of R_K, where $B(0, r) = \{x : ||x||_2 \le r\}$,

$$R_K = \frac{\varepsilon(0)}{\lambda_{\max}(P)}, \; I_K = \frac{||A_K(0)^{-1}||_2 \lambda^2_{\max}(P)}{\varepsilon(0)\lambda_{\min}(P)} \tag{30}$$

and P is positive define matrix satisfying $P{=}P^T > 0$ and

$$A_K(0)^T P + P A_K(0) + \varepsilon(0) I \le O \tag{31}$$

Proof. Substituting the differential form of the MIMO-PI controller

$$\dot{u}(t) = K_P \dot{x}(t) + K_I x(t) \tag{32}$$

into the velocity form of perturbed autonomous system [34]

$$\ddot{x}(t) = \frac{\partial f}{\partial x}\dot{x}(t) + \frac{\partial f}{\partial u}\dot{u}(t) + \dot{d} \tag{33}$$

to obtain the state-space model of $s(t) = (\dot{x}(t), x(t))^T$ considering the perturbed term $d_s = (\dot{d}^T, 0^T)^T$ as

$$\begin{pmatrix} \ddot{x}(t) \\ \dot{x}(t) \end{pmatrix} = \begin{pmatrix} \frac{\partial f}{\partial x} + \frac{\partial f}{\partial u} K_P & \frac{\partial f}{\partial u} K_I \\ I_n & O \end{pmatrix} \begin{pmatrix} \dot{x}(t) \\ x(t) \end{pmatrix} + \begin{pmatrix} \dot{d} \\ 0 \end{pmatrix} \tag{34}$$

$$\iff \dot{s}(t) = f_s(s(t)) + d_s = A_K(s(t))s(t) + d_s \tag{35}$$

Furthermore, we can simplify the Jacobian of $f_s(0)$ according to the Lemma 4 that

$$\frac{\partial f_s(0)}{\partial x} = A_K(0) \; is \; stable \tag{36}$$

Hence, according to Lemma 1, there exists $P{=}P^T > 0$ and $\varepsilon(0) > 0$ such that

$$\left[\frac{\partial f_s(0)}{\partial x}\right]^T P + P\left[\frac{\partial f_s(0)}{\partial x}\right] + \varepsilon(0) I \le O \tag{37}$$

Let $\Omega = \{0\}$, according to Theorem 1 and Remark 2, as $t \to \infty$

$$s(t) \to S(0) = \left\{ x : ||A_K(0)x||_2 \le \frac{2L_d L_f \lambda_{\max}^2(P)}{\varepsilon(0)\lambda_{\min}(P)} \right\} \tag{38}$$

Given that $Re[A_K(0)] < 0$, it follows that $A_K(0)$ is non-singular, and consequently, there exists a set

$$S^* = \left\{ x : ||x||_2 \le \frac{2L_d L_f ||A_K(0)^{-1}||_2 \lambda_{\max}^2(P)}{\varepsilon(0)\lambda_{\min}(P)} \right\} \tag{39}$$

such that $s(t) \to S(0) \subset S^*$. Thus, the proof is completed. □

Remark 3. It is worth noting that when $L_d \to 0$, the system's final state $s(t)$ will converge exponentially to zero, which precisely demonstrates its robust stability. Meanwhile, this also indirectly verifies that the MIMO-PI controller can effectively stabilize the linearized system near the equilibrium point, thereby achieving global exponential stabilization for the corresponding nonlinear system.

Meanwhile, it also should be noted that $A_K(0)$ can be described as a linear combination of the coefficients K_P and K_I as follows

$$A_K(0) = D_1(0) + D_2(0)K \tag{40}$$

where

$$K = (K_P, K_I) \tag{41}$$

and

$$D_1(0) = \begin{pmatrix} \frac{\partial f(0)}{\partial x} & O \\ I_n & O \end{pmatrix},\ D_2(0) = \begin{pmatrix} \frac{\partial f(0)}{\partial u} \\ O \end{pmatrix} \tag{42}$$

4.2. Robust convergency indicator

From the perspective of Theorem 2, two indices R_K and I_K are introduced to characterize the convergence performance of the MIMO-PI controller. Specifically, R_K quantifies the exponential convergence rate of the error, while I_K delineates the range of the ultimate convergent global random attractor of the error. The relationship between I_K and R_K is characterized by

$$I_K = \frac{\tau(P_K)}{R_K \sigma_{\min}(A_K(0))} \tag{43}$$

where

$$\tau(P_K) = \frac{\lambda_{\max}(P_K)}{\lambda_{\min}(P_K)},\ R_K = \frac{\varepsilon(0)}{\lambda_{\max}(P_K)} \tag{44}$$

and subject to

$$A_K(0)^T P_K + P_K A_K(0) + \varepsilon(0) I \le O \tag{45}$$

Furthermore, a larger R_K implies a faster error convergence rate, which is prone to inducing oscillations. Counterintuitively, an excessively large R_K does not necessarily guarantee that the system error will eventually converge to a smaller global random attractor. The ultimate global random attractor range I_K of the error during the convergence process is influenced by three factors: the condition number $\tau(P_K)$ of the positive definite matrix P_K, the exponential convergence rate R_K, and the minimum spectral norm $\sigma_{\min}(A_K(0))$ of $A_K(0)$.

4.3. The calculation of indicator

We aim to compute the corresponding R_K and I_K values for any given K_P and K_I, which would allow us to screen out the optimal coefficients K_P and K_I for the MIMO-PI controller in any perturbed nonlinear system. The key point, and indeed the first step, of this problem is how to calculate R_K. Since it is coupled with both the positive definite matrix P_K and the margin $\varepsilon(0)$, computing its exact value poses a challenge. To tackle this issue, we introduce the positive definite matrix $Q = Q^T > 0$ associated with P as follows, which serves as the starting point for computing R_K.

$$Q_K = \frac{P_K}{\varepsilon(0)} \tag{46}$$

Thus, we can present the relationship between R_K and Q_K as follows:

$$R_K = \frac{1}{\lambda_{\max}(Q_K)} \tag{47}$$

subject to

$$A_K(0)^T Q_K + Q_K A_K(0) + I \le O \tag{48}$$

In fact, there are theoretically numerous, even infinitely many, such Q_K. We thus adopt an optimistic estimation: specifically, we take the value of R_K^* as our actual R_K, where R_K^* corresponds to Q_K^*-the element that maximizes R_K within the set defined by Eq. (48). Under this framework, the solution for Q_K^* is reduced to a type of eigenvalue problem (EVP) as follows:

$$Q_K^* = \text{argmin}_{Q_K = Q_K^T > 0} \gamma \tag{49}$$

$$s.t. \begin{cases} Q_K \le \gamma I \\ A_K(0)^T Q_K + Q_K A_K(0) + I \le O \end{cases} \tag{50}$$

Upon obtaining Q_K^*, we can then compute R_K and I_K as follows:

$$R_K = \frac{1}{\lambda_{\max}(Q_K^*)} \tag{51}$$

$$I_K = \frac{\tau(Q_K^*)}{R_K \sigma_{\min}(A_K(0))} \tag{52}$$

4.4. Optimization model of controller coefficients

Our primary objective is to determine the optimal gain coefficients for the MIMO-PI controller. Specifically, under the constraints of a predefined exponential convergence rate R^*, a given initial value $x(t_0) = x_0$, and input limitations as specified in Eq. (25), we aim to maximize the achievement of the optimization objective outlined in Eq. (23). This optimization model can be characterized by the indices R_K and I_K as follows

$$\max_K R_K$$
$$s.t. \begin{cases} I_K \le I^* \\ u_{\min} \le u_K(t_0) \le u_{\max} \\ \dot{u}_{\min} \le \dot{u}_K(t_0) \le \dot{u}_{\max} \end{cases} \tag{53}$$

where let sampling time $\Delta t = 0.1s$, and

$$u_K(t_0) = K \begin{pmatrix} x_0 \\ x_0 \Delta t \end{pmatrix}, \ \dot{u}_K(t_0) = K \begin{pmatrix} 0 \\ x_0 \end{pmatrix} \tag{54}$$

The aforementioned optimization model represents a canonical constrained nonlinear optimization problem (NP), which can be effectively addressed using algorithms such as the classical genetic algorithm (GA) to determine the optimal controller coefficients. Solving this model solely requires knowledge of the initial state of the perturbed system and the Jacobian matrix evaluated at the system's equilibrium point; explicit information regarding the disturbance type or the detailed system structure is not necessary. Furthermore, this approach obviates the need for extensive model simplification, a distinct advantage that facilitates its implementation in model-free engineering applications.

5. Simulation verification

In this section, we first verify the correctness of our proposed theoretical framework, specifically Theorem 1. Building upon this, we further validate the rationality of the robust convergence indicator proposed for the MIMO-PI controller through comparative experiments with different controller parameters.

5.1. The correctness of the Theorem 1

We will verify the validity of Theorem 1 for classical perturbed nonlinear autonomous system in this subsection, such as Duffing model. The Duffing model [35] is a nonlinear vibration model proposed by the German physicist Rudolf Duffing in the early 20th century. This model describes the vibration behavior of systems with nonlinear restoring forces and finds extensive applications in physics, engineering, biology, chaos theory, and other fields, particularly for studying bifurcation, chaos, and resonance characteristics in nonlinear systems. The Duffing model without external driving force and subject to bounded perturbation d_F can be described as:

$$\ddot{x} + \delta \dot{x} + \alpha x + \beta x^3 = d_F, \ ||d_F||_2 \le L_d \tag{55}$$

where x denotes the deformation of the damped nonlinear oscillator, while α, β, and δ represent the corresponding structural parameters. The corresponding perturbed nonlinear state-space model is described as follows:

$$\begin{cases} \dot{x}_1 = x_2 \\ \dot{x}_2 = -\delta x_2 - \alpha x_1 - \beta x_1^3 + d_F \end{cases} \tag{56}$$

Table 2
Hyperparameter declarations.

Declaration	Param	Value	Unit
Simulation timespan	T	[0,20]	s
Acceleration of gravity	g	9.81	m/s^2
Consolidated velocity	V	25	m/s
Initial climb angle	$\gamma(0)$	$\pi/4$	rad
Initial azimuth angle	$\chi(0)$	$\pi/3$	rad
Initial roll angle	$\phi(0)$	$\pi/3$	rad
Initial overload	$n_z(0)$	1	–
Reference climb angle	γ_c	$\pi/12$	rad
Reference azimuth angle	χ_c	0	rad
Reference roll angle	ϕ_c	0	rad
Reference overload	n_{zc}	0	–
Lipschitz constant of d_χ	L_{d_χ}	0.1	–
Lipschitz constant of d_γ	L_{d_γ}	0.1	–
Disturbance frequency of d_χ	ω_χ	0.15	rad/s
Disturbance frequency of d_γ	ω_γ	0.15	rad/s
The range of ϕ	$[\phi_{\min},\phi_{\max}]$	$[-\pi/4,\pi/4]$	rad
The range of $\dot{\phi}$	$[\dot{\phi}_{\min},\dot{\phi}_{\max}]$	$[-\pi/6,\pi/6]$	rad/s
The range of n_z	$[n_{z,\min},n_{z,\max}]$	[-2.1,2.1]	–
The range of $\dot{n}_z$	$[\dot{n}_{z,\min},\dot{n}_{z,\max}]$	[-1,1]	$/s$

The Jacobian of the above unperturbed system can be expressed as:

$$J_D(f) = \begin{pmatrix} 0 & 1 \\ -\alpha - 3\beta x_1^2 & -\delta \end{pmatrix} \tag{57}$$

According to Theorem 1 and Remark 2, we can configure appropriate α, β, and δ such that when $(x_1, x_2) = (0, 0)$, the Jacobian

$$J_D(f(0)) = \begin{pmatrix} 0 & 1 \\ -\alpha & -\delta \end{pmatrix} \tag{58}$$

satisfies the following condition that, there exist a positive-definite matrix $P(0) = P(0)^T > 0$ and $\varepsilon(0) > 0$ such that

$$J_D(f(0))^T P(0) + P(0) J_D(f(0)) + \varepsilon(0) I \leq O \tag{59}$$

A sufficient condition is:

$$\lambda_{\max}(J_D(f(0))) < 0 \iff \alpha > 0, \delta > 0 \tag{60}$$

Then as $t \to \infty$, $x(t)$ would converge exponentially to

$$S(0) = \{x : ||f(x)||_2 \leq \frac{2L_d ||J_D(f(0))||_2 \lambda_{\max}^2(P(0))}{\varepsilon(0)\lambda_{\min}(P(0))}\} \tag{61}$$

at least the rate of $\varepsilon(0)/\lambda_{\max}(P(0))$. Next, we will conduct multiple sets of comparative experiments to verify this point. As illustrated in Fig. 1, subfigure (a) validates the robust stability of the autonomous system under disturbances. Subfigure (b) compares convergence performance across different parameters α and exponential convergence rates. Subfigures (c) and (d) quantitatively characterize the results from subfigure (b), with (c) and (d) respectively illustrating how $R(f)$ and $I(f)$ influence the mean and standard deviation of $\|f(x)\|_2$.

5.2. The optimizable MIMO-PI controller

To validate the designed optimizable robust controller, its feasibility is verified herein through the simplified kinematic model [36] of a fixed-wing aircraft in the ground coordinate system along the γ and χ directions as follows

$$\begin{aligned} \dot{\chi}(t) &= \frac{g \tan\phi(t)}{V} + d_\chi \\ \dot{\gamma}(t) &= \frac{g(n_z(t)\cos\phi(t) - \cos\gamma(t))}{V} + d_\gamma \end{aligned} \tag{62}$$

where the physical state of the kinematic model considered in this study using $x(t) = (\chi(t), \gamma(t))^T$, and the input command $u(t) = (\phi(t), n_z(t))^T$ signifies the vector containing roll angle $\phi(t)$ and normal overload $n_z(t)$ along the z-axis direction. $d = (d_\chi, d_\gamma)^T$ is the disturbance term caused by factors such as wind field and model simplification applied to $\dot{\chi}(t)$ and $\dot{\gamma}(t)$ respectively. Here the perturbation d is given in the form of sinusoidal noise signal as

$$d_\chi = L_{d_\chi} \sin(\omega_\chi t), d_\gamma = L_{d_\gamma} \cos(\omega_\gamma t) \tag{63}$$

We declare critical hyperparameters for this experiment in Table 2. It is stipulated that the initial derivative of all states are zero. Subsequently, we respectively utilize the underlying:

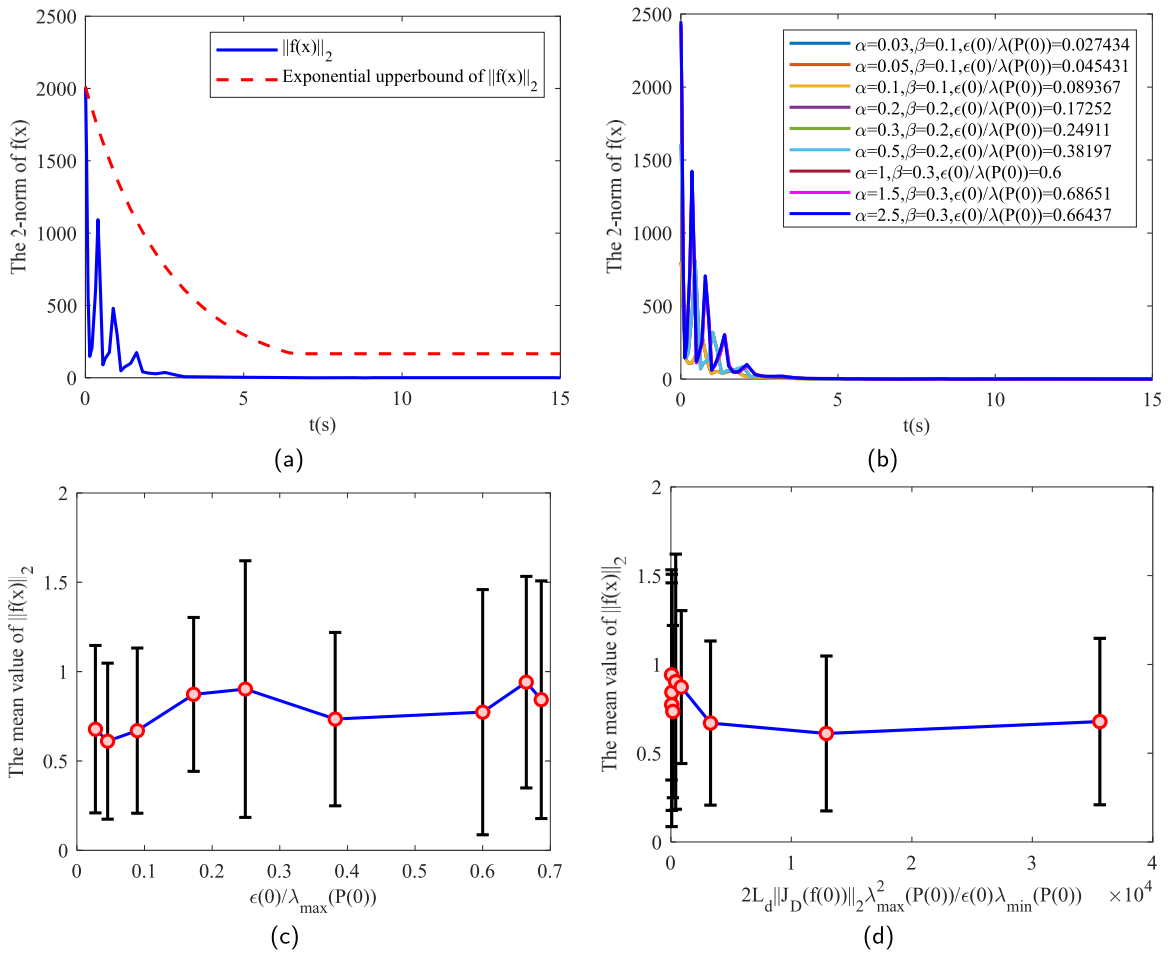

Fig. 1. For multiple sets of simulation experiments on the Duffing model. (a): Curves of $\|f(x)\|_2$ and its exponential upperbound versus time for $\alpha = 0.5$, $\beta = 0.25$, $\delta = 1.5$, $L_d = 2.5$; (b): Time-series curves of $\frac{\epsilon(0)}{\lambda_{\max}(P(0))}$ and $\|f(x)\|_2$ for different α and β; (c): Curves of the mean and standard deviation of $\|f(x)\|_2$ for different $\frac{\epsilon(0)}{\lambda_{\max}(P(0))}$; (d): Curves of the mean and standard deviation of $\|f(x)\|_2$ for different $\frac{2L_d\|J_D(f(0))\|_2\lambda^2_{\max}(P(0))}{\epsilon(0)\lambda_{\min}(P(0))}$.

- Average Integral Time Absolute Error(ITAE, the average of the absolute differences between the actual signal and the reference signal, integrated over a specific time period);
- Peak Time(PT, the time it takes for a signal to rise from a defined initial value to its highest point);
- Maximum Overshoot (MO, the maximum deviation by which a response exceeds its final value)
- Mean value after Stabilization (MS, the mean value of convergence errors in the last 1/4 time interval)
- Standard deviation after Stabilization (ST, the standard deviation of convergence errors in the last 1/4 time interval)

to quantify the performances of MIMO-PI controller under different circumstances. Assuming that the velocity of aircraft is well-maintained to V, and g denotes the gravitational acceleration, which equals to 9.81m/s^2. Define the reference tracking signals as $x_c = (\chi_c, \gamma_c)^T$ with the tracking error $e(t) = (e_\chi(t), e_\gamma(t))^T$ as

$$e(t) = x_c - x(t) = (\chi_c - \chi(t), \gamma_c - \gamma(t))^T \tag{64}$$

Under this specific form of error, the above perturbed system under the constrain $\dot{x}_c = 0$ is transformed into:

$$\dot{e}(t) = f_e(e(t), u(t)) + d_e \tag{65}$$

where $d_e = (-d_\chi, -d_\gamma)^T$ and

$$f_e(e(t), u(t)) = \begin{pmatrix} -\frac{g\tan\phi(t)}{V} \\ -\frac{g(n_z(t)\cos\phi(t) - \cos(\gamma_c - e_\gamma(t)))}{V} \end{pmatrix} \tag{66}$$

The Jacobians of $f_e(e, u)$ with respect to e and u are:

$$\frac{\partial f_e(e,u)}{\partial e} = \begin{pmatrix} 0 & 0 \\ 0 & \frac{g}{V}\sin(\gamma_c - e_\gamma) \end{pmatrix} \tag{67}$$

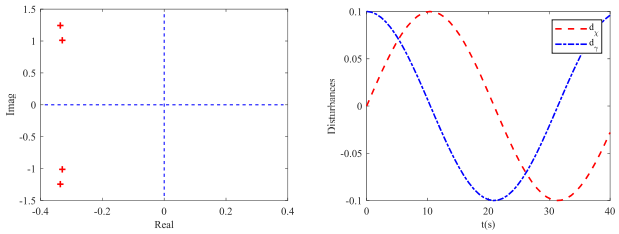

Fig. 2. The eigenvalue distribution at the origin and the applied sinusoidal disturbance d_χ, d_γ. (a): Eigenvalue distribution; (b): d_χ, d_γ.

$$\frac{\partial f_e(e,u)}{\partial u} = \begin{pmatrix} -\frac{g}{V}\sec^2\phi & 0 \\ \frac{gn_z}{V}\sin\phi & -\frac{g}{V}\cos\phi \end{pmatrix} \tag{68}$$

The Jacobians of the above equation at the equilibrium point $e_\gamma = 0$, $e_\chi = 0$, $\phi = 0$, and $n_z = \cos\gamma_c / g$ are:

$$\frac{\partial f_e(0)}{\partial e} = \begin{pmatrix} 0 & 0 \\ 0 & \frac{g}{V}\sin\gamma_c \end{pmatrix}, \frac{\partial f_e(0)}{\partial u} = \begin{pmatrix} -\frac{g}{V} & 0 \\ 0 & -\frac{g}{V} \end{pmatrix} \tag{69}$$

For stabilizing the above perturbed system, we design a MIMO-PI controller in the following form as

$$u(t) = K_P e(t) + K_I \int_0^t e(t)dt \tag{70}$$

The optimal K_P^* and K_I^* computed by solving the Eq. (53) using GA optimization method are:

$$K_P^* = \begin{pmatrix} 1.6968 & 0.5906 \\ -0.5906 & 1.9556 \end{pmatrix}$$
$$K_I^* = \begin{pmatrix} 3.4869 & 0.1784 \\ -0.1784 & 3.4869 \end{pmatrix} \tag{71}$$

where the corresponding convergence indictors are as follows

$$R_K^* = 0.4427,\ I_K^* = 4.9244 \tag{72}$$

5.2.1. The effect of error stabilization

In the case of the current optimal coefficients K_p^* and K_I^*, the eigenvalue distribution of $A_K(0)$ corresponding to the MIMO-PI controller is shown in Fig. 2(a), from which it can be observed that all eigenvalues lie in the left half of the complex plane. The applied sinusoidal disturbance signal is presented in Fig. 2(b).

Under the MIMO-PI controller corresponding to K_P^* and K_I^*, the time-series curves of tracking errors e_χ, e_γ, $\dot{e}_\chi$, and $\dot{e}_\gamma$ are illustrated in Fig. 3. It can be observed that e_χ and e_γ rapidly converge to a very small region near the origin within 20 s. During this process, the maximum overshoot of e_χ does not exceed 0.8 rad, and that of e_γ is within 0.4 rad, with their maximum peak time less than 4 s. It is also noteworthy that the input command curves under these controller parameters are presented in Fig. 4, which indicate that the commands satisfy the corresponding input constraints.

5.2.2. The influence of R_K and I_K

To validate the rationality of using indices R_K and I_K for quantifying robust stability during error convergence, we derive new controller coefficients K by introducing incremental perturbations ΔK to the baseline optimal coefficients $K^* = (K_P^*, K_I^*)$.

$$K = K^* + \Delta K \tag{73}$$

We then compare the corresponding response curves and their associated performance metrics-ITAE, MO, PT, MS, and ST-across multiple such coefficient sets. For simplicity, ΔK can be described in the following form

$$\Delta K = -\varepsilon(I_p, I_i) \tag{74}$$

where I_p and I_i both are identity matrixes for standard form $m = n$, and $\epsilon \in \mathbb{R}^1$ is served as a regulation variable to determine ΔK.Table 3

Subsequently, we analyzed the dynamic response, as depicted in Fig. 5. The result indicates that across multiple channels, a higher R_K correlates with superior exponential convergence. Conversely, it's more likely to cause oscillation and a lack of convergence when a small R_K occurs. This is because a larger R_K tends to indicate a higher exponential convergence rate, causing the error energy to decay more rapidly throughout the convergence process-specifically, with smaller amplitudes and slower oscillation frequencies. In a sense, R_K exerts a significantly more pronounced influence on steady-state error and convergence performance than I_K.

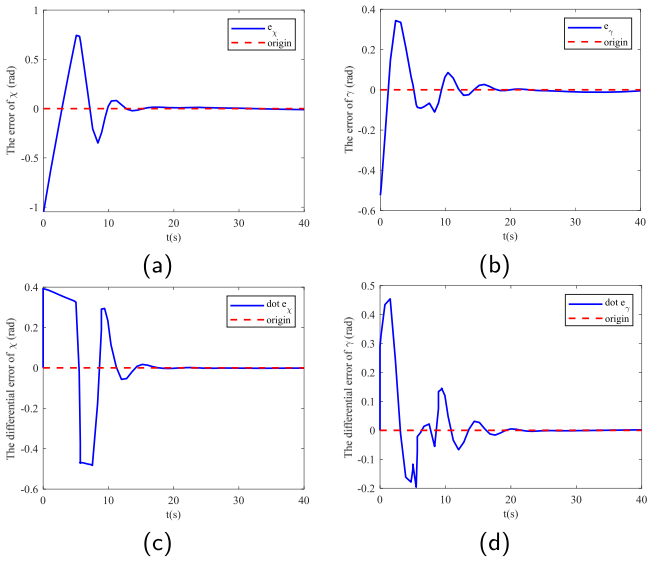

Fig. 3. Error stabilization profiles comparsion under the MIMO-PI controller using R_K^* and I_K^* for e_γ, e_χ, $\dot{e}_\gamma$ and $\dot{e}_\chi$. (a): $e_\chi(t)$ profile; (b): $e_\gamma(t)$ profile; (c): $\dot{e}_\chi(t)$ profile; (d): $\dot{e}_\gamma(t)$ profile.

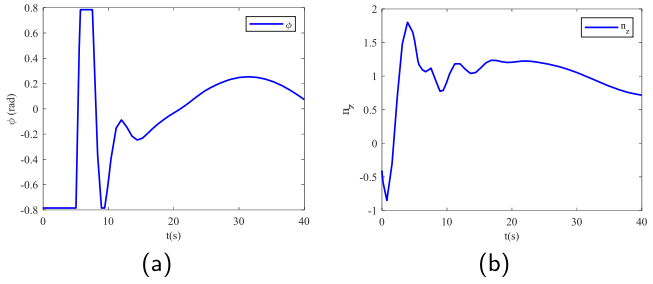

Fig. 4. Input commands for MIMO-PI controller within coefficients R_K^* and I_K^*. (a): $\phi(t)$ profile; (b): $n_z(t)$ profiles.

Table 3
The different ε and corresponding R_K, I_K.

Type	ε	$R(f)$	$I(f)$	Type	ε	$R(f)$	$I(f)$
K_1	−4	0.7742	7.873	K_4	0.5	0.3626	5.207
K_2	−2	0.6754	6.057	K_5	0.8	0.2849	6.161
K_3	−1	0.5913	5.312	K_6	1	0.2192	8.258

The trend profiles quantitatively illustrating the relationship between the R_K and various performance metrics including ITAE, MO, and PT are depicted in Fig. 6, the comparsion of performance MS, ST on

$$s_\chi = \sqrt{e_\chi^2 + \dot{e}_\chi^2},\ s_\gamma = \sqrt{e_\gamma^2 + \dot{e}_\gamma^2} \tag{75}$$

are presented in Fig. 7. Specifically, higher R_K corresponds to lower ITAE, MS and ST for all errors e_χ, e_γ, $\dot{e}_\chi$, $\dot{e}_\gamma$. Furthermore, in most cases, larger R_K tends to correlate with smaller MO and PT, translating to a reduced maximum overshoot and a shorter peak time.

Specifically, to explore how R_K and I_K influence the convergence processes of e_χ and e_γ, we analyzed the effects of R_K and I_K respectively on the mean values and standard deviations of the errors e_χ, e_γ, and their derivatives $\dot{e}_\chi$, $\dot{e}_\gamma$ during convergence, as illustrated in Fig. 8. Notably, comparisons between subfigures (b), (d) and (f), (h) reveal that the influences of R_K and I_K on e_χ and e_γ originate from their actions on $\dot{e}_\chi$ and $\dot{e}_\gamma$. As shown by the comparison of subfigures (c) and (g), the effects of I_K and R_K on the mean values of the error derivatives $\dot{e}_\chi$ and $\dot{e}_\gamma$ are relatively minor (on the order of 10^{-3} only). Meanwhile, comparisons of subfigures (d) and (h) indicate that R_K has a significant impact on the standard deviations of $\dot{e}_\chi$ and $\dot{e}_\gamma$ during convergence-specifically, R_K exhibits an approximately inverse relationship with these standard deviations. This implies that a larger R_K can notably reduce oscillations during convergence and enhance the quality of robust convergence.

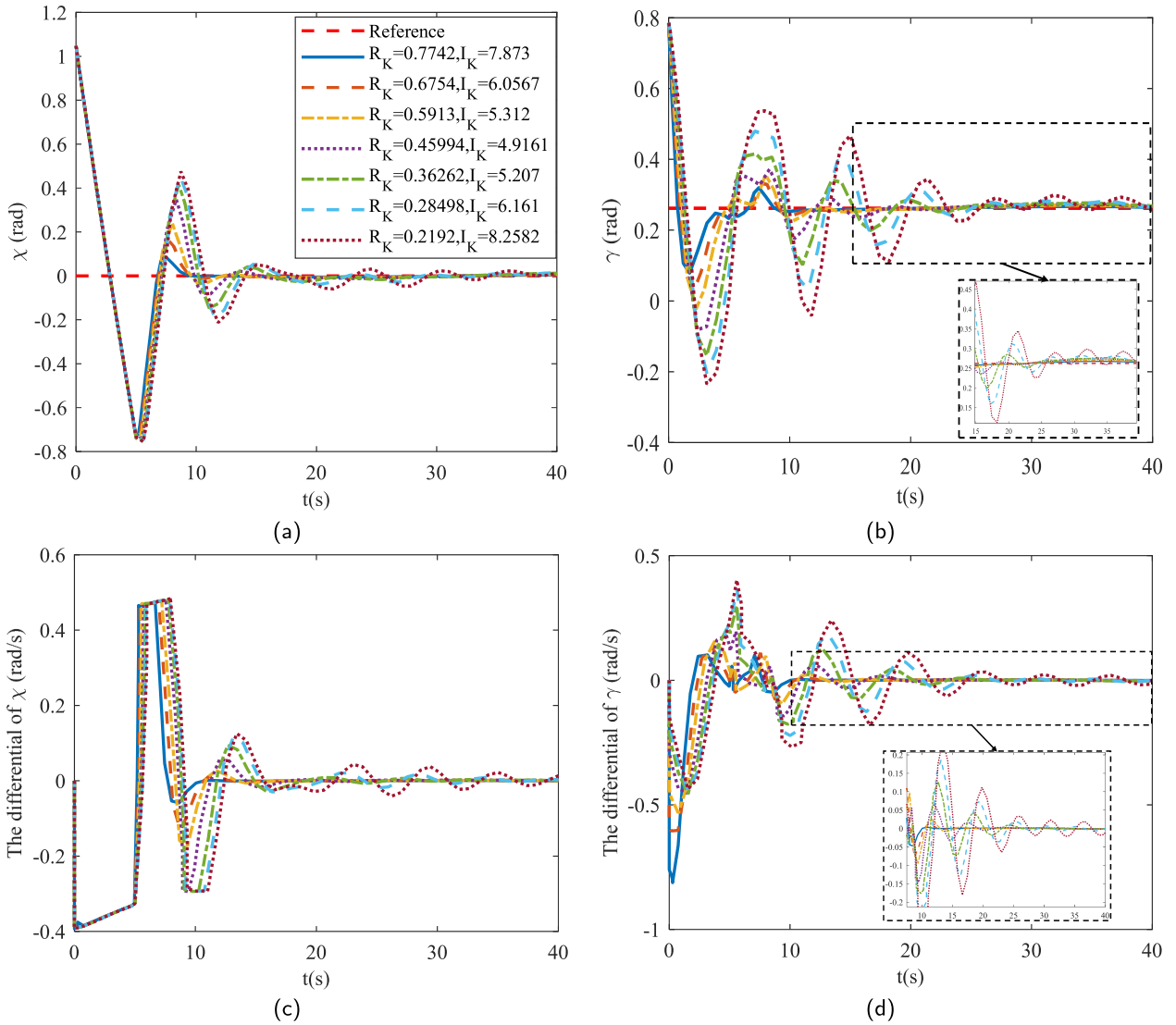

Fig. 5. Profiles comparsion of γ, χ, $\dot{\gamma}$ and $\dot{\chi}$ accompanied by different ϵ within coresponding R_K and I_K. (a): Comparison of response profiles for R_K, I_K on χ; (b): Comparison of response profiles for R_K, I_K on γ; (c): Comparison of response profiles for R_K, I_K on $\dot{\chi}$; (d): Comparison of response profiles for R_K, I_K on $\dot{\gamma}$.

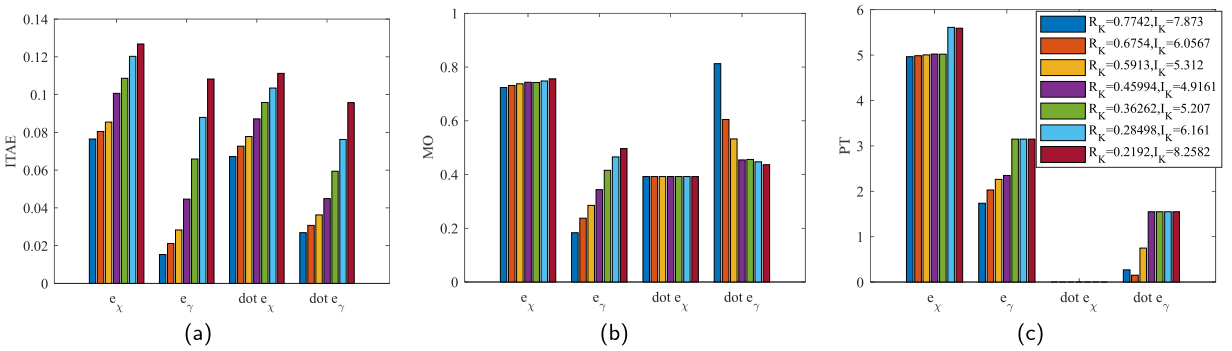

Fig. 6. Performance indicators comparison of ITAE, MO and PT between multiple corresponding R_K, I_K respectively for e_γ, e_χ, $\dot{e}_\gamma$ and $\dot{e}_\chi$. (a): The comparison of ITAE; (b): The comparison of MO; (c): The comparison of PT.

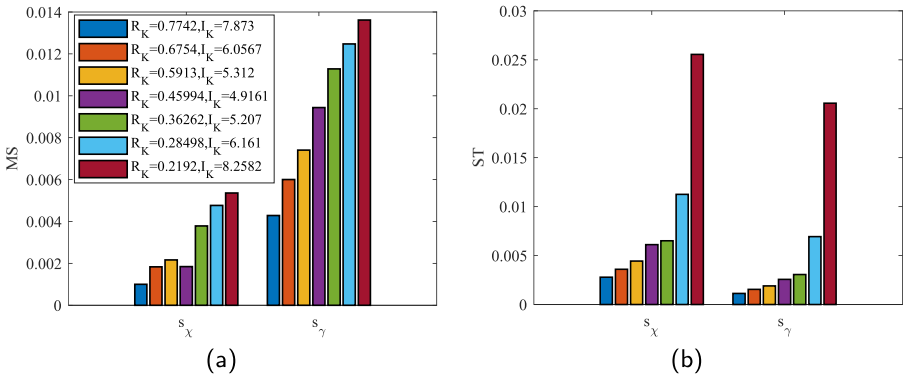

Fig. 7. Comparison of MS and ST for states s_χ and s_γ under robust indices R_K and I_K corresponding to different ε. (a): Comparison of MS; (b): Comparison of ST.

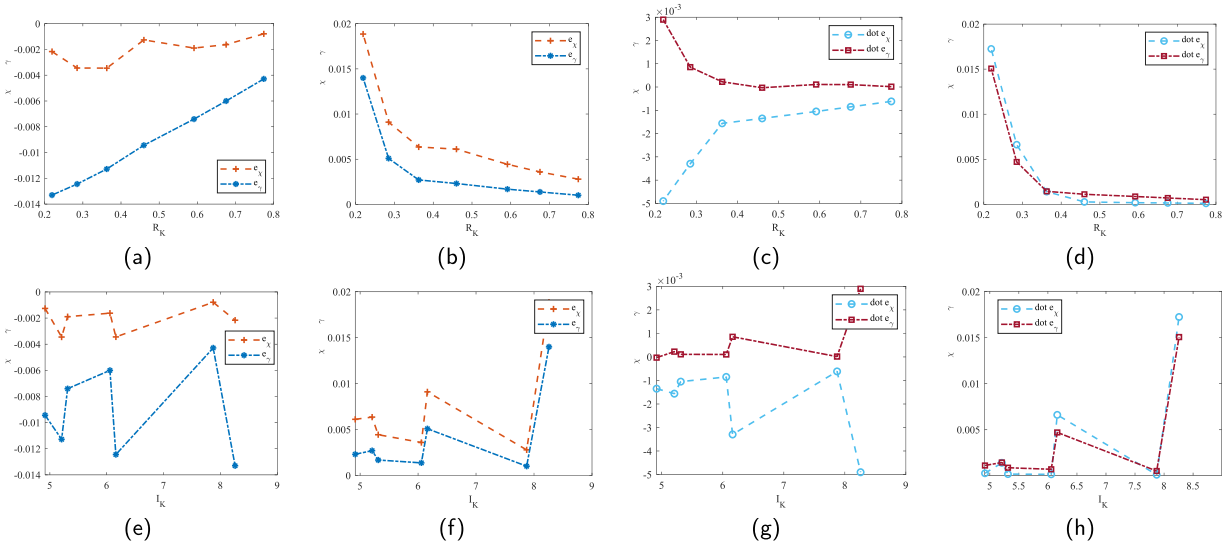

Fig. 8. This figure illustrates the relationships of the average value and standard deviation indices for e_γ, e_χ, $\dot{e}_\gamma$, and $\dot{e}_\chi$ with respect to the variations of R_K and I_K. (a): The average values comparsion of e_γ and e_χ with respect to R_K; (b): The standard deviations comparsion of e_γ and e_χ with respect to R_K; (c): The average values comparsion of $\dot{e}_\gamma$ and $\dot{e}_\chi$ with respect to R_K; (d): The standard deviations comparsion of $\dot{e}_\gamma$ and $\dot{e}_\chi$ with respect to R_K; (e): The average values comparsion of e_γ and e_χ with respect to I_K; (f): The standard deviations comparsion of e_γ and e_χ with respect to I_K; (g): The average values comparsion of $\dot{e}_\gamma$ and $\dot{e}_\chi$ with respect to I_K; (h): The standard deviations comparsion of $\dot{e}_\gamma$ and $\dot{e}_\chi$ with respect to I_K.

In a word, the largest R_K signifies an overall enhancement of comprehensive performance during the error stabilization process, as a larger R_K reduces the energy of error derivatives during convergence, mitigates the oscillatory nature of errors in the exponential convergence process, and thus enhances the quality of robust stability.

5.2.3. *The analysis of robustness*

To evaluate the robust performance of the MIMO-PI controller under significant disturbances with different amplitudes and frequencies, we adopt the controller coefficients K_P^* and K_I^* and test its performance against disturbances characterized by various amplitudes L_d and frequencies ω_d listed in Table 4 as follows

$$L_{d_\chi} = L_{d_\gamma} = L_d,\ \omega_\chi = \omega_\gamma = \omega_d \tag{76}$$

The response curves of e_χ, e_γ, $\dot{e}_\chi$, and $\dot{e}_\gamma$ under different disturbances are presented in Fig. 9. It can be observed that nearly all response curves stabilize in the vicinity of the origin after 20 s. Notably, as disturbance intensity increases (i.e., with larger L_d and ω_d), the overshoot of e_χ decreases, while the post-20-s disturbance amplitudes of both e_χ and e_γ increase accordingly. During this error stabilization process, despite the fact that larger L_d and ω_d amplify the disturbance energy, the MIMO-PI controller effectively mitigates the impact of this energy, achieving robust stability near the origin to the greatest extent possible.

On the other hand, we quantified the ITAE, MS, and ST metrics under varying disturbances, as illustrated in Fig. 10. First, analyzing from the ITAE perspective, it is observed that for disturbances with $L_d = 0.1$ and 0.3, increasing the disturbance frequency ω_d does not result in a significant rise in ITAE; in fact, there is even a decreasing trend. This indicates that the MIMO-PI controller's performance

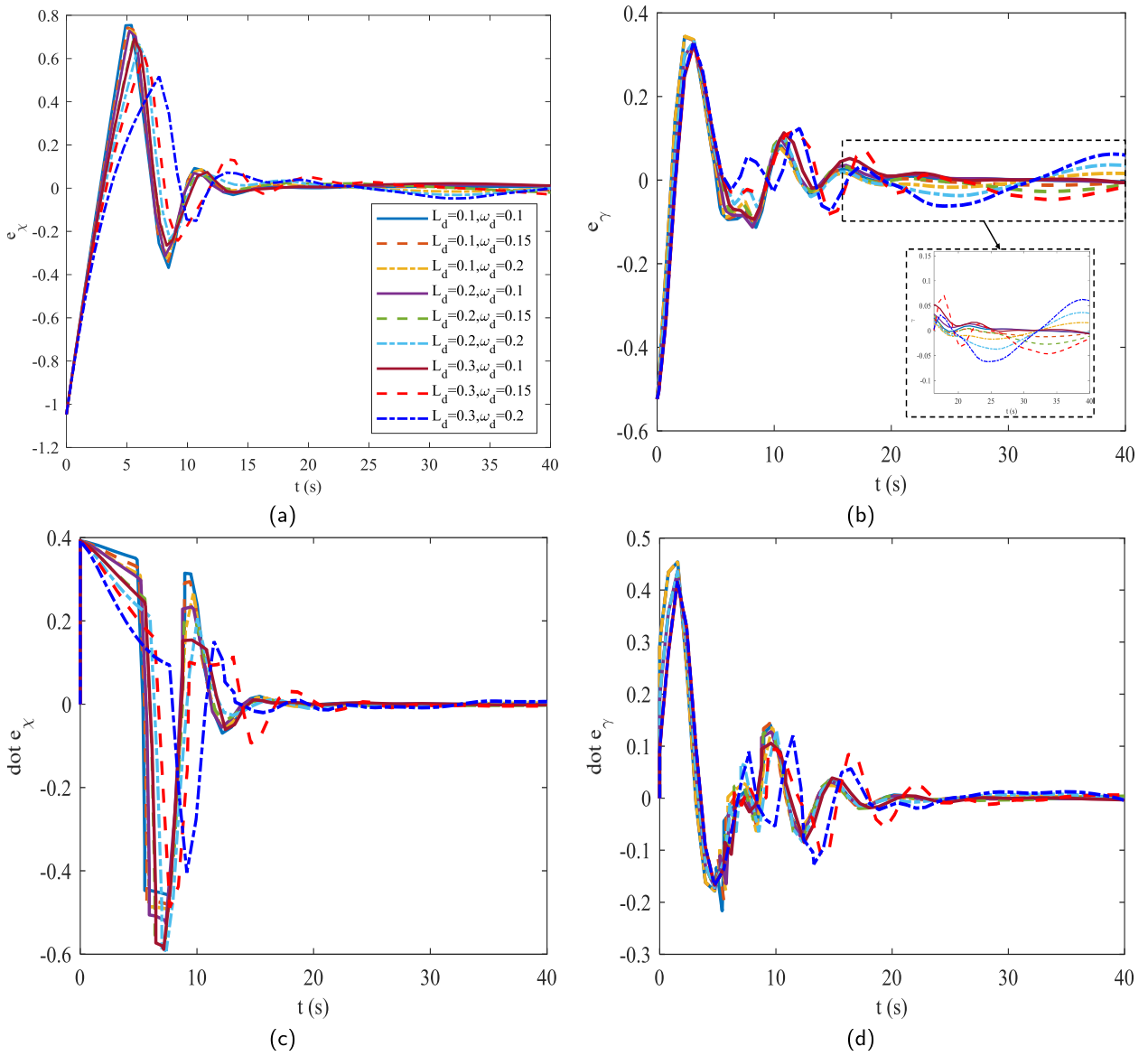

Fig. 9. Error profiles comparsion of γ, χ, $\dot{\gamma}$ and $\dot{\chi}$ under different L_d and ω_d. (a): Comparison of response profiles on e_χ; (b): Comparison of response profiles on e_γ; (c): Comparison of response profiles on $\dot{e}_\chi$; (d): Comparison of response profiles on $\dot{e}_\gamma$.

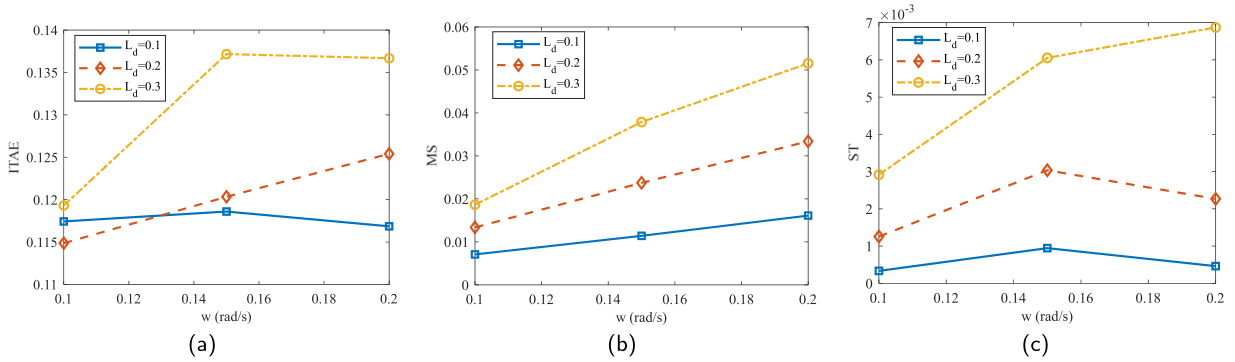

Fig. 10. Comparison of ITAE, MS, and ST corresponding to different disturbance amplitudes L_d and frequencies ω. (a) Comparison of ITAE; (b) Comparison of MS; (c) Comparison of ST.

Table 4
The L_d and ω_d for different disturbances.

Type	L_d	ω_d	Type	L_d	ω_d	Type	L_d	ω_d
d_1	0.1	0.1	d_2	0.1	0.15	d_3	0.1	0.2
d_4	0.2	0.1	d_5	0.2	0.15	d_6	0.2	0.2
d_7	0.3	0.1	d_8	0.3	0.15	d_9	0.3	0.2

is insensitive to increases in disturbance frequency, reflecting its superior capability in suppressing high-frequency offsets. Second, from the MS standpoint, increasing ω_d and L_d enhances the disturbance-induced impact on steady-state performance. Fortunately, this impact exhibits linearity, which prevents excessively intense disturbances from triggering abrupt transitions or chaotic behaviors. Finally, regarding ST: while an increase in L_d leads to a rise in ST, the magnitude of this steady-state standard deviation growth is minimal (on the order of 10^{-3}). Similarly, as ω_d increases, ST shows no pronounced upward trend, indicating that the controller's steady-state oscillation is also insensitive to ω_d increments. This underscores its excellent performance in suppressing high-frequency oscillations.

Conclusions and future work

In this study, we put forward the critical quantitative metrics for assessing robustness in the context of general perturbed nonlinear system and validate its effectiveness. The specific research work is as follows:
(1) From the perspective of global random attractor, an innovative theoretical framework is proposed to quantify the stability performance of autonomous nonlinear disturbed systems;
(2) Building upon this theoretical framework, robust convergence indices R_K and I_K for quantifying MIMO-PI controllers are developed;
(3) A set of controller coefficient optimization methods is established to optimize the robust convergence indices.

Experimental results validate the correctness of the proposed theory, the effectiveness of the indices, and the optimality of the controller. Subsequent research should concentrate on two primary aspects:
(1) exploring methods to configure the eigenvalue distribution of $A_K(0)$ in order to attain an optimal robust indicator;
(2) investigating strategies to guarantee quadratic optimization of the error and input command through judicious parameter tuning while maintaining exponential convergence.

CRediT authorship contribution statement

Zimao Sheng: Writing – review & editing, Writing – original draft, Visualization, Software, Methodology, Investigation, Data curation, Conceptualization; **Hong'an Yang:** Supervision, Resources, Project administration, Funding acquisition; **Jiakang Wang:** Writing – review & editing, Validation; **Tong Zhang:** Writing – review & editing, Formal analysis.

Declaration of competing interest

The authors declare that they have no known competing financial interests or personal relationships that could have appeared to influence the work reported in this paper.

References

[1] K.J. Åström, T. Hägglund, PID control, IEEE Control Syst. Mag. 1066 (2006) 30–31.
[2] T. Samad, A survey on industry impact and challenges thereof [technical activities], IEEE Control Syst. Mag. 37 (1) (2017) 17–18.
[3] T.L. Blevins, PID advances in industrial control, IFAC Pro. Volumes 45 (3) (2012) 23–28.
[4] C.-G. Kang, Origin of stability analysis:\" on governors\" by JC Maxwell [historical perspectives], IEEE Control Syst. Mag. 36 (5) (2016) 77–88.
[5] B.B. Alagoz, F.N. Deniz, M. Koseoglu, An efficient PID-based optimizer loop and its application in De Jong's functions minimization and quadratic regression problems, Syst. Control Lett. 159 (2022) 105090.
[6] A. O'dwyer, Handbook of PI and PID Controller Tuning Rules, World Scientific, 2009.
[7] J.G. Ziegler, N.B. Nichols, Optimum settings for automatic controllers, Trans. Am. Soc. Mech. Eng. 64 (8) (1942) 759–765.
[8] L.H. Keel, S.P. Bhattacharyya, Controller synthesis free of analytical models: three term controllers, IEEE Trans. Automat. Control 53 (6) (2008) 1353–1369.
[9] N.J. Killingsworth, M. Krstic, PID tuning using extremum seeking: online, model-free performance optimization, IEEE Control Syst. Mag. 26 (1) (2006) 70–79.
[10] C. Zhao, L. Guo, Towards a theoretical foundation of PID control for uncertain nonlinear systems, Automatica 142 (2022) 110360.
[11] C. Zhao, L. Guo, Control of nonlinear uncertain systems by extended PID, IEEE Trans. Automat. Control 66 (8) (2020) 3840–3847.
[12] L. Guo, C. Zhao, Control of nonlinear uncertain systems by extended PID with differential trackers, Commun. Inf. Syst. 21 (3) (2021) 415–440.
[13] G. Zames, B. Francis, Feedback, minimax sensitivity, and optimal robustness, IEEE Trans. Automat. Control 28 (5) (1983) 585–601.
[14] R. Vilanova, A. Visioli, PID Control in the Third Millennium, 75, Springer, 2012.
[15] D.E. Rivera, M. Morari, S. Skogestad, Internal model control: PID controller design, Ind. Eng. Chem. Process Des. Dev. 25 (1) (1986) 252–265.
[16] K.J. Åström, T. Hägglund, Automatic tuning of simple regulators with specifications on phase and amplitude margins, Automatica 20 (5) (1984) 645–651.
[17] O. Arrieta, R. Vilanova, Simple PID tuning rules with guaranteed Ms robustness achievement, IFAC Proc. Volumes 44 (1) (2011) 12042–12047.
[18] Y.-D. Son, S.-D. Bin, G.-G. Jin, Stability analysis of a nonlinear PID controller, Int. J. Control Autom. Syst. 19 (2021) 3400–3408.
[19] B. Verma, P.K. Padhy, Robust fine tuning of optimal PID controller with guaranteed robustness, IEEE Trans. Ind. Electron. 67 (6) (2019) 4911–4920.
[20] C. Zhao, L. Guo, PID controller design for second order nonlinear uncertain systems, Sci. China Inf. Sci. 60 (2017) 1–13.

[21] X. Cong, L. Guo, PID control for a class of nonlinear uncertain stochastic systems, in: 2017 IEEE 56th Annual Conference on Decision and Control (CDC), IEEE, 2017, pp. 612–617.
[22] J. Zhang, L. Guo, PID control for high dimensional nonlinear uncertain stochastic systems, in: 2019 Chinese Control Conference (CCC), IEEE, 2019, pp. 1501–1505.
[23] X. Yu, P. Ding, L. Ou, W. Zhang, General stabilization approach of the low-order controller for both SISO systems and MIMO systems with multiple time delays, Automatica 166 (2024). https://doi.org/10.1016/j.automatica.2024.111639
[24] H. Wang, L.A. Ricardez-Sandoval, A deep reinforcement learning-based PID tuning strategy for nonlinear MIMO systems with time-varying uncertainty, IFAC Papersonline 58 (14) (2024) 887–892. 12th IFAC Symposium on Advanced Control of Chemical Processes (ADCHEM), Toronto, CANADA, JUL 14–17, 2024. https://doi.org/10.1016/j.ifacol.2024.08.449
[25] S.K. Pandey, A novel optimum decoupling and control of MIMO systems based on linear matrix inequality and Kharitonov theorem, Eng. Lett. 33 (5) (2025) 1671–1683.
[26] B. Djaballah, C. Nouibat, R. W. Ayad, Optimization of fractional-order PI-PID controllers for MIMO systems using artificial bee colony algorithm, Soft. Comput. 28 (2024) 10281–10299. https://doi.org/10.1007/s00500-024-09776-y
[27] L. Cavanini, R. Felicetti, F. Ferracuti, A. Monteriu, Error governor for active fault tolerance in PID control of MIMO systems, Int. J. Syst. Sci. 56 (7) (2025) 1457–1473. https://doi.org/10.1080/00207721.2024.2427850
[28] F. Gopmandal, A. Ghosh, A hybrid search based script capital H_∞ synthesis of static output feedback controllers for uncertain systems with application to multivariable PID control, Int. J. Robust Nonlinear Control 31 (12) (2021) 6069–6090. https://doi.org/10.1002/rnc.5581
[29] S. Zhong, Y. Huang, L. Guo, An ADRC-based PID tuning rule, Int. J. Robust Nonlinear Control 32 (18, SI) (2022) 9542–9555. https://doi.org/10.1002/rnc.5845
[30] K. Xiang, Y. Song, P. Ioannou, Nonlinear adaptive PID control for nonlinear systems, IEEE Trans. Automat. Control (2025) 1–8. https://doi.org/10.1109/TAC.2025.3567565
[31] J. Zhu, C. Zhao, PID Control of MIMO nonlinear uncertain systems with low relative degrees, IEEE Control Syst. Lett. 8 (2024) 3213–3218. https://doi.org/10.1109/LCSYS.2024.3524056
[32] A.J. Van Schaft, L_2-gain analysis of nonlinear systems and nonlinear state-feedback H_∞ control, IEEE Trans. Autom. Control 37 (6) (1992) 770–784.
[33] R.A. Horn, C.R. Johnson, Matrix analysis, Cambridge university press, 2012.
[34] D.J. Leith, W.E. Leithead, Gain-scheduled and nonlinear systems: dynamic analysis by velocity-based linearization families, Int. J. Control 70 (2) (1998) 289–317. https://doi.org/10.1080/002071798222415
[35] A.H. Salas Salas, J.E. Castillo Hernandez, L.J. Martinez Hernandez, The duffing oscillator equation and its applications in physics, Math. Probl. Eng. 2021 (2021). https://doi.org/10.1155/2021/9994967
[36] A. Samir, H.M. Calderon, H. Werner, B. Herrmann, F. Thielecke, Predictive path-following control for fixed-wing UAVs using the qLMPC framework in the presence of wind disturbances, in: AIAA SciTech 2024 Forum, AIAA, 2024. AIAA SciTech Forum, Orlando, FL, JAN 08–12, 2024.